Macromolecules
ARTICLE

Macromolecules **2009**, *42*, 4449–4455 **4449**
DOI: 10.1021/ma9006494

Expanding the Realm of Furan-Based Conducting Polymers through Conjugation with 1,6-Methano[10]annulene

Patricia A. Peart[†] and John D. Tovar*[,†,‡]

[†]*Department of Chemistry and* [‡]*Department of Materials Science and Engineering, Johns Hopkins University, 3400 N. Charles Street, NCB 316, Baltimore, Maryland 21218*

Received March 26, 2009; Revised Manuscript Received May 13, 2009

ABSTRACT: The synthesis of a new bisfuranyl monomer, 2,7-bis(2-furanyl)-1,6-methano[10]annulene, is presented. Its properties and those of its polymer, synthesized via electropolymerization, are compared to those of the known furan−arene−furan monomers and their respective polymers. Investigation using UV−vis spectroscopy, cyclic voltammetry, and spectroelectrochemistry indicated that the 1,6-methano[10]annulene copolymer has properties rivaling those of the copolymers containing traditional aromatic cores. These results are rationalized in conjunction with DFT calculations, and they further the premise that 1,6-methano[10]annulene can be viewed as a viable building block for advanced π-conjugated electronic materials.

Introduction

Polymers containing five-membered heterocyclic rings such as thiophene and pyrrole are frequently investigated as organic semiconductors owing to their favorable electronic properties and weaker aromaticity relative to benzene. However, furan is often overlooked in this field due to the difficulty involved in synthesizing truly conjugated polyfurans. Although furan has less aromatic stabilization energy, in practice it is harder to oxidize than thiophene and pyrrole and as such suffers from side reactions during chemical and electrochemical polymerization. Nevertheless, polymers that consist of furan rings continue to be investigated for potential use as organic semiconductors.[1] This may be linked to the fact that furan is a readily available "green material" produced during the breakdown of rice hulls and that polyfuran has desirable properties such as electrochromicity and good redox ability.[2] The electrical resistivity of polyfuran decreases significantly but reversibly upon contact with moisture, rendering these materials important for potential use as humidity sensors.[3] Conjugated polymers built with furan derivatives have shown promise as blue organic light-emitting diodes (OLEDs),[4] and theoretical work suggests that polyfuran could be n-doped leading to higher n-channel electron mobility than that found in polypyrrole.[5]

Polyfuran (and other polyaromatics) was synthesized in the presence of catalytic trichloro- or trifluoroacetic acid.[6] This and other acid-catalyzed syntheses of polyfuran[1] did not yield conjugated polymers due to the formation of various hydrogenated forms of furan within the polymer backbone. Furan is generally accepted as the least aromatic of the heterocyclic compounds mentioned above, thereby rendering its oxidized intermediates more reactive and more prone to side reactions such as ring addition, oxidation, and cleavage.[7] This results in polymers containing tetrahydrofuranyl rings, aliphatic carbonyl portions, and other defects as illustrated in Figure 1.[8,9]

Polyfuran was initially synthesized via anodic oxidation by Tourillon and Garnier.[10] However, Zotti et al. showed that some furan monomers were irreversibly oxidized during electropolymerization, resulting in a polymer that was not polyconjugated.[8] The latter group produced polyconjugated polyfuran via the electroreduction of 2,5-dibromofuran. However, the conductivity of this polyconjugated polyfuran turned out to be very low.[8] Wan et al. lowered the oxidation potential of furan by using the boron trifluoride−ethyl ether complex as the solvent.[11] They determined using FT-IR and Raman spectroscopy that while this resulted in the polymer having less ring-opened content, it was still not fully polyconjugated. In addition to chemical and electrochemical synthesis, other synthetic methods have been employed, but truly conjugated polyfuran remains elusive.[1]

One of the problems with synthesizing polyfuran *chemically* lies with the insolubility of the polymer thus formed while the potential required for monomer *electropolymerization* is high and typically results in destructive ring-opening of the furanyl units that make up the polymer. To lower the oxidation potential required for electrochemical polymerization, the conjugation of the monomer could be extended by coupling with additional unsaturated units. An example is the synthesis of polyfuran from terfuran (**FFF**) by Glenis et al.[12] as synthesized from 1,4-bis(2-furanyl)-1,4-butanedione. The oxidation potential of **FFF** was ~1.5 V (vs SCE) less positive than that of furan. The properties of the polymers obtained seemed to depend on the electrolyte used (i.e., dopant). 2,5-Bis(2-furanyl)thiophene (**FTF**) was prepared and electrochemically polymerized by Galal et al.[13] Their investigation revealed that the monomer oxidation potential of **FTF** was less positive than that of furan by ~0.74 V (vs Ag/AgCl). The oxidation potential of the polymers followed a similar trend. The conductivity of $NOPF_6$-doped poly(**FTF**) and poly(**TFT**) was determined by Joshi et al. using the four-probe dc method.[14] Poly(**FTF**) exhibited the lower conductivity at $< 10^{-5}$ S/cm while poly(**TFT**) had conductivity of 0.2 S/cm. A series of conducting polymers derived from 1,4-bis(2-furanyl)benzene (**FBF**) were synthesized by Reynolds et al.[15] Theoretical work by Hong and Marynick predicted that these **FBF** monomers would be coplanar and therefore more fully conjugated.[16] The monomer oxidation potential for these molecules proved to be lower than that of furan, and the conductivities of the resulting poly(**FBF**)s were all on the scale of 10^{-1} S/cm when electrochemically oxidized in the presence of ClO_4^- and measured using a four-probe method. The

*Corresponding author. E-mail: tovar@jhu.edu.

Published on Web 06/05/2009

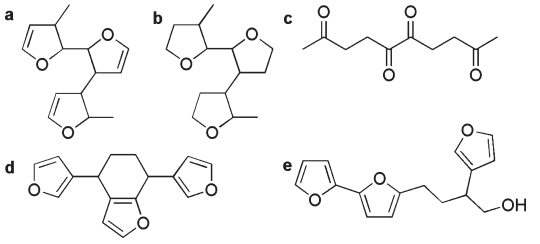

Figure 1. Representative defect structures in polyfuran: (a) branching and partial saturation, (b) complete saturation forming tetrahydrofuran rings, (c) ring-opening leading to aliphatic carbonyls,[8] (d, e) other ring-opened segments.[9]

polymer films formed showed no carbonyl functionality when examined by FT-IR, suggesting that little or no ring-opening occurred. More recently, other bisfuranyl monomers containing central 2,5-pyrrole,[17] 4,4′-biphenyl,[18] carbazole, and fluorene[19] have been investigated toward synthesizing copolymers of furan.

We recently reported new conjugated polymers that contain the 10π electron aromatic 1,6-methano[10]annulene.[20,21] Thienyl-annulene monomers were polymerized and shown to have favorable electrochemical properties when compared to their benzenoid counterparts. The 2,7-bis(2-thiophenyl)-1,6-methano-[10]annulene (**TMT**) had an oxidation potential of 0.97 V (vs Ag/Ag^+) in 0.1 M TBAP/CH_2Cl_2; under the same conditions we determined that α-terthiophene (**TTT**) had an oxidation potential of 1.24 V. When the 2,7-disubstituted 1,6-methano[10]annulene monomers and polymers were compared to their 1,5-disubstituted naphthyl counterparts, the compounds containing the annulene 10π electron ring had less positive oxidation potentials and more stable radical cations than the benzenoid 10π electron molecules. Additionally, spectroelectrochemical data pointed to greater extended conjugation in the methano[10]annulyl polymers in their charged conductive states. In this report, we expand on the use of 1,6-methano[10]annulene as applied to furan-based conductive polymers through the synthesis and electropolymerization of 2,7-bis(2-furanyl)-1,6-methano[10]annulene (**FMF**). The bisfuranyl compounds and their polymers were investigated using UV−vis spectroscopy, DFT calculations (B3LYP/6-31G*), cyclic voltammetry, spectroelectrochemistry, and in situ conductivity measurements.

Results and Discussion

Monomer Syntheses. Previously, we demonstrated that thiophene-appended annulenes, once polymerized into conjugated polymers, offered materials with greater delocalization than their corresponding naphthalene counterparts.[20] Here, we prepared furan-appended derivatives of the annulene (**FMF**) and the naphthalene (**FNF**). **FMF** and **FNF** were synthesized via Stille couplings carried out under nitrogen using dimethylformamide (DMF) as the solvent and tetrakis(triphenylphosphino)palladium(0) as the catalyst (Scheme 1). Three known bisfuranyl monomers, namely, 1,4-bis(2-furanyl)benzene (**FBF**), 2,5-bis(2-furanyl) thiophene (**FTF**), and α-terfuran (**FFF**), were synthesized in the same manner and were investigated for the purpose of comparison (Scheme 1). We report literature values for established optical and electrochemical data when appropriate but draw all conclusions from data collected here under uniform experimental conditions. The structure and purity of the monomers were confirmed by ^{1}H NMR, ^{13}C NMR, and mass spectrometry. For the previously synthesized monomers, the NMR data were consistent with literature values.

Monomer UV−vis Spectra. The UV−vis spectrum for each furan monomer was obtained in chloroform (Figure 2).

Scheme 1. Synthesis of Monomers

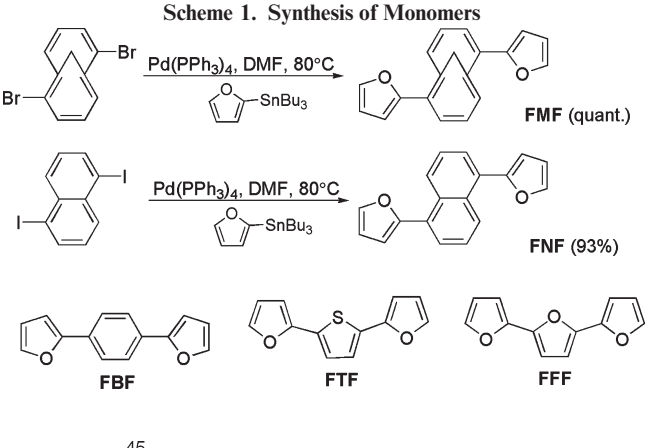

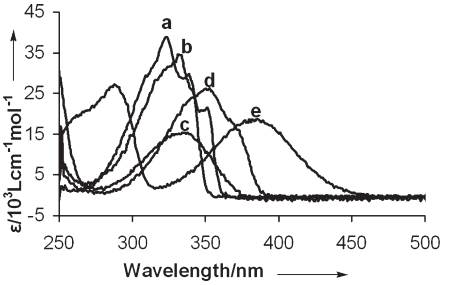

Figure 2. UV−vis spectra of the furan-containing monomers taken in chloroform at room temperature: (a) **FBF**, (b) **FFF**, (c) **FNF**, (d) **FTF**, (e) **FMF**.

The monomer demonstrating the greatest maximum wavelength of absorption (λ_{max}) at 384 nm was **FMF**, thus revealing that it has the smallest HUMO−LUMO gap. The thiophenyl monomer **FTF** had the closest λ_{max} to that of **FMF** at 370 nm. The λ_{max} of the other monomers ranged between 334 nm (**FNF** and **FBF**) and 351 nm (**FFF**). This data is not exactly in keeping with the theoretical trends calculated for the bandgap using the DFT B3LYP/6-31G* method (Table 2). From the DFT calculations **FBF** would be expected to have the lowest λ_{max} with **FNF** and **FFF** having similar λ_{max}. However, for the onset of absorptions, the trend follows that of theory, with onsets of 450 nm for **FMF**, 390 nm for **FTF**, 375 nm for **FNF**, 361 nm for **FFF**, and 355 nm for **FBF** (Table 1).

Electropolymerization. The monomers were electrochemically polymerized on Pt electrodes using cyclic voltammetry. In the first scan of each, a single oxidation peak for the formation of the monomer radical cation was observed, and in subsequent scans, anodic features indicative of polymer growth appeared at less positive potential. With each scan, the current for both features increased, representative of the deposition of electroactive material on the electrode surface. All electrochemical data are quoted versus a *quasi*-internal Ag/Ag^+ reference electrode under conditions listed in the respective figures.

The lowest anodic monomer oxidation peak (E_{pa}) was observed at 0.65 V for both **FMF** and **FFF**. The E_{pa} of **FTF** (see Supporting Information) was recorded in this work at 0.69 V (Galal et al. reported as 0.81 vs Ag/AgCl in ACN with $TBABF_4$ as the supporting electrolyte[13]), and **FBF** had an E_{pa} of 0.84 V (which is not far from the E_{pa} of 0.78 V (vs Ag/Ag^+) reported by Reynolds et al.[15] using $TBAClO_4$ electrolyte). **FNF** exhibited the highest E_{pa} at 0.98 V due to the lack of delocalization through the naphthalene core, in line with our previous work.[20,21] During monomer oxidation, an electron is removed from the HOMO of the neutral monomer by the metal electrode. This experimental trend in

Table 1. Experimental Data for Furanyl Monomers

monomer	λ_{max} (nm)	onset λ (nm)	HOMO−LUMO gap (eV)[a]	HOMO (eV)[b]
FMF	386	450	2.76	−4.43
FNF	335	375	3.31	−4.70
FTF	330	390	3.18	−4.45
FBF	315	355	3.49	−4.60
FFF	331	361	3.43	−4.43

[a] Calculated using the energy associated with the onset of absorption. [b] Determined by cyclic voltammetry from the onset of anodic current in the first scan of the electropolymerization.

Table 2. Results of DFT B3LYP/6-31G* Calculations for Furanyl Monomers

monomer	HOMO (eV)	LUMO (eV)	HOMO−LUMO gap (eV)
FMF	−4.99	−1.58	3.41
FNF	−5.21	−1.40	3.81
FTF	−5.00	−1.38	3.62
FBF	−5.14	−1.18	3.96
FFF	−4.91	−1.05	3.86

oxidation potential (both for onset of oxidation and for the E_{pa}) is corroborated by the theoretical values calculated for the HOMO of these monomers (Table 2), although the higher calculated HOMO of **FFF** would imply a less positive monomer oxidation. All the furanyl comonomers showed E_{pa} that were significantly lower than that of just furan (1.7 V vs Ag/Ag^+) with the **FMF** monomer being the same as that with the lowest oxidation potential thus far, **FFF** (Figure 3). It is important to note that during electropolymerization **FMF** appears not to grow as efficiently as the other monomers. This could be a consequence of enhanced solubility of the radical cation formed after monomer oxidation due to the nonplanar annulene geometry.

Polymer Electronics. Once the polymer was synthesized, the polymer-coated electrode was rinsed with monomer-free electrolyte and used to obtain the cyclic voltammogram of the polymer. For each of these polymers, the peak current appears to vary linearly with the scan rate, which indicates that there is indeed an electroactive species bound to the electrode. The polymer obtained from the electropolymerization of **FFF** had the least positive anodic oxidation peak at 0.50 V (previously reported as 0.74 V vs SCE using the same supporting electrolyte).[12] This was closely followed by the E_{pa} of poly(**FMF**) and poly(**FTF**) (see Supporting Information) both at 0.52 V [in the case of poly(**FTF**) Galal et al. reported the E_{pa} as 0.80 V vs Ag/AgCl].[13] Poly(**FNF**) had an E_{pa} 70 mV higher at 0.59 V, again consistent with our earlier findings that showed how the naphthalene with this connectivity had higher redox potentials. Poly(**FBF**) seemed to have two anodic peaks: one small prepeak at 0.39 V and the other at 0.62 V (Reynolds et al. reported only a single oxidation peak at 0.60 V vs Ag/Ag^+ but with $TBAClO_4$ as the supporting electrolyte)[15] (Figure 4). All appear to be electrochemically reversible with profiles befitting of conductive polymers. As noted in the previous section, **FMF** did not polymerize as efficiently as the other polymers, so it is possible that poly(**FMF**) polymers have shorter chain lengths.

Spectroelectrochemistry. The polymers of each furan-containing monomer were grown on ITO-coated glass electrodes from 5 mM solutions in 0.1 M n-Bu_4NPF_6/CH_2Cl_2. These electrodes were rinsed after the polymer growth and placed in monomer-free electrolyte in quartz cuvettes in order to record UV−vis spectra while changing the potential applied to the film.

The neutral polymer λ_{max} was longest for poly(**FMF**) at 445 nm and shortest for poly(**FNF**) at 342 nm. This suggests that poly(**FMF**) has the smallest HOMO−LUMO gap and

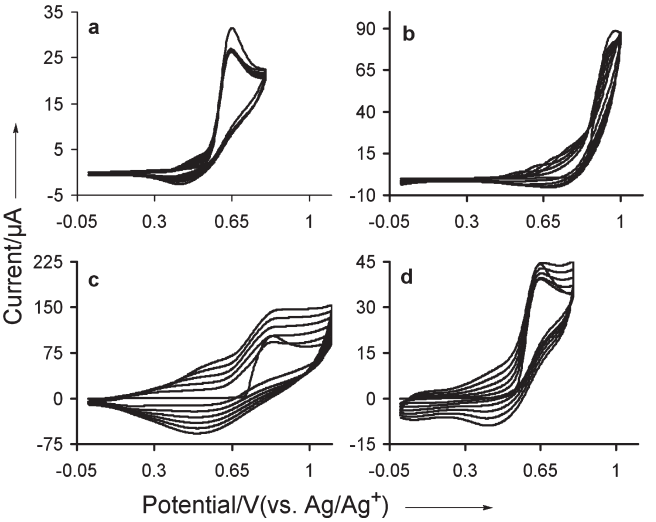

Figure 3. Polymer growth profiles of the furan-containing monomers (a) **FMF**, (b) **FNF**, (c) **FBF**, and (d) **FFF** on 1.6 mm diameter Pt button electrode in 5 mM solutions of each monomer in 0.1 M n-Bu_4NPF_6/MeCN at 100 mV/s scan rate.

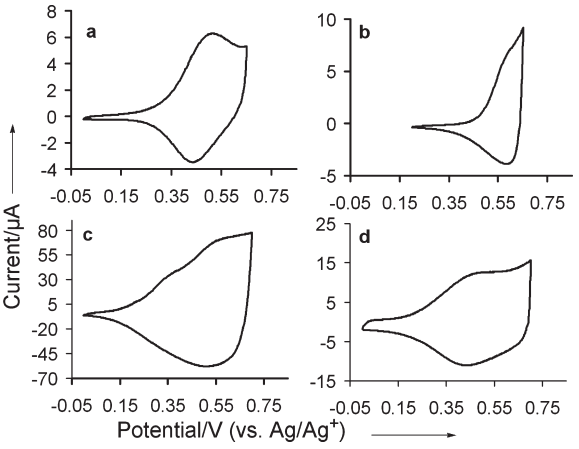

Figure 4. Cyclic voltammograms of polymer films of (a) poly(**FMF**), (b) poly(**FNF**), (c) poly(**FBF**), and (d) poly(**FFF**) on 1.6 mm diameter Pt button electrode taken in 0.1 M n-Bu_4NPF_6/MeCN at 100 mV/s scan rate.

the longest effective conjugation length as expected for a system with a higher degree of intramolecular delocalization. The spectral signatures for poly(**FMF**) in the neutral and the oxidized states were also the broadest, which we attribute to the possibility of having differing absorbing species with varying effective conjugation lengths throughout the polymer in the thin electrodeposited solid film. This behavior was observed in our earlier work with annulene−oligothiophene copolymers.[20] The absorption profiles for all the other polymers were narrower, suggestive of more well-defined electronic structures. The benzene-containing polymer had the next highest and broadest neutral polymer λ_{max} of 405 nm

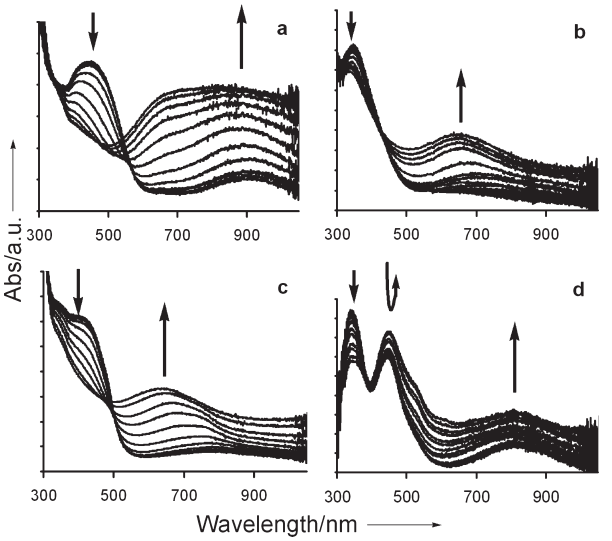

Figure 5. Spectroelectrochemical data for (a) poly(**FMF**), (b) poly(**FNF**), (c) poly(**FBF**), and (d) poly(**FFF**) grown on ITO-coated glass electrodes and recorded in 0.1 M n-Bu_4NPF_6/CH_2Cl_2 at 100 mV/s. The arrows show how the absorption profile evolves as the applied electrochemical potential is increased anodically.

[Reynolds et al. reported a peak at 3.2 eV (387 nm) in 0.1 M $TBAClO_4$ in MeCN].[15] With the exception of poly(**FMF**), all polymers had what seemed to be very localized polaronic transitions when compared to the broad absorption associated with the charged states of poly(**FMF**) (Figure 5).

Another interesting observation is the persistence of the neutral peaks for poly(**FNF**), poly(**FFF**), and poly(**FTF**) [see Supporting Information for poly(**FTF**)] as the potential at which the polymer is held is increased. This is in contrast to the neutral peaks of poly(**FMF**) and poly(**FBF**) which were no longer present upon the application of higher potentials. This suggests that the structures of poly(**FNF**), poly(**FTF**), and poly(**FFF**) are more localized than those of poly(**FMF**) and poly(**FBF**), even after oxidation and injection of mobile charge carriers. The persistent localized peaks were present both in very thick and in optically transparent thin films, suggesting that this is not merely an issue of inefficient charge compensation or incomplete film oxidation. The minimal shift observed between the absorption maximum of **FNF** and the neutral absorption maximum of poly(**FNF**) is in line with our previous work wherein we deduced that naphthyl copolymers had shorter effective conjugation lengths than those of the corresponding annulenyl copolymers due to electronic localization in the naphthyl systems.[20] A bathochromic shift of 17 nm is observed between the absorption maximum of **FFF** and the neutral absorption maximum of poly(**FFF**). This slight shift may be an indication of a lack of conjugation throughout the polymer possibly due to polymer degradation. This would also be consistent with the persistence of the neutral peak in these polymers at higher potentials. We noted that poly(**FFF**) spectroelectrochemical data did not vary significantly with film thickness.

Conductivity Measurements. Qualitative in situ conductivity measurements, for poly(**FMF**), poly(**FBF**), and poly(**FFF**), were obtained, where the polymer to be investigated was electropolymerized on interdigitated Au electrodes leading to eventual coverage of the entire array of the device. A small potential difference (V_D) of 40 mV was maintained across the two microelectrodes during the CV experiment, and the potentials (V_G) of both electrodes were varied versus the reference electrode (0.01 M Ag/Ag^+ in MeCN) at the same scan rate. For a conductive polymer, a drain current (I_D) will flow between the two electrodes once the polymer has been doped into a conductive state. The magnitude of the current is directly proportional to the conductivity of the polymer. Therefore, plotting the graph of I_D vs V_G gives relative conductivities at specific points along the polymer cyclic voltammogram.[22,23]

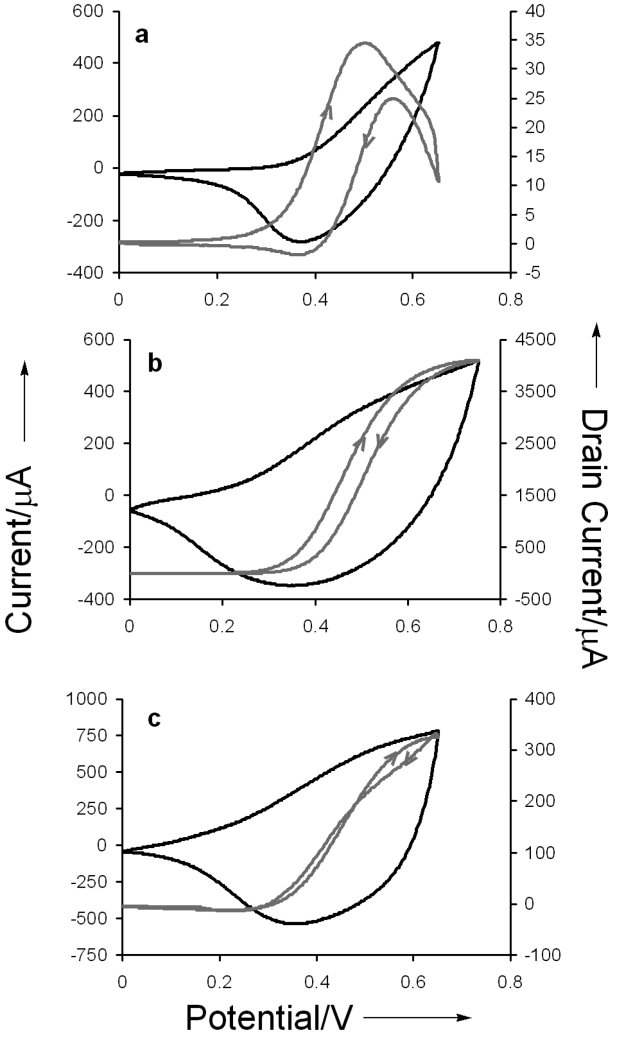

Figure 6. Cyclic voltammograms (black curves) and conductivity measurements (gray curves) of (a) poly(**FMF**), (b) poly(**FBF**), and (c) poly(**FFF**) obtained on interdigitated Au electrodes in 0.1 M n-Bu_4NPF_6/MeCN. CVs acquired at 100 mV/s scan rates while the drain current measurements were taken at 5 mV/s scan rates.

For poly(**FMF**) and poly(**FFF**) the potentials of the microelectrodes were varied from 0.00 to 0.65 V, while for poly(**FBF**) the potential of the microelectrodes was varied from 0.00 to 0.75 V. It was determined that all three furanyl polymers became conductive once the polymer was oxidized (Figure 6). For poly(**FMF**), conductivity was observed between 0.25 and 0.65 V. Its conductivity reached a maximum at around 0.50 V but began to decline at more positive potentials. There is some difference in conductivity between the positive and negative sweep for poly(**FMF**) wherein the maximum conductivity of the negative sweep is lower than that for the positive sweep. The magnitude of maximum I_D was not reproducible on subsequent sweeps; in fact, it decreased significantly, and so the difference between the positive and negative sweeps could be attributed to irreversible degradation of the poly(**FMF**) under the experimental conditions. Poly(**FBF**) was conductive between 0.28 and

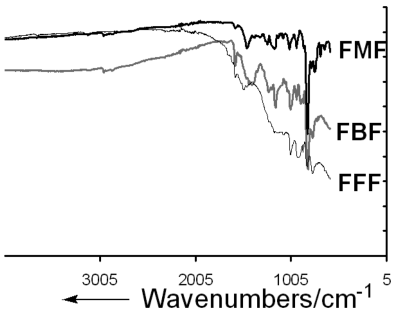

Figure 7. ATR-IR spectra for undoped poly(**FMF**) (thick black), poly(**FBF**) (thin black), and poly(**FFF**) (gray) that were first grown on an ITO-coated glass electrode in 0.1 M n-Bu_4NPF_6/MeCN at 100 mV/s scan rate.

0.75 V. Its conductivity reached a maximum at 0.69 V and remained there for the rest of the positive sweep (to 0.75 V). The magnitude of the maximum I_D decreased slightly on subsequent scans, and so it can be assumed that some polymer degradation occurs in this sweep range. Poly(**FFF**) was conductive between 0.28 and 0.65 V. Its maximum conductivity was reached at 0.60 V and remained there for the rest of the positive sweep (to 0.65 V). The magnitude of maximum I_D was reproducible on subsequent scans, and therefore it may be deduced that no degradation of poly (**FFF**) occurs within this sweep range. However, when the potential sweep width was extended out to 0.70 V, degradation became evident (not shown). Unfortunately, we were unable to obtain meaningful data for poly(**FNF**) due to poor electrochemical growth on the inderdigitated array. Given that the data provides only qualitative conductivity, it is not possible to deduce the better conductor, but we can conclude that all three were conductive. It is interesting to note that the poly(**FBF**) grew easily and created a thicker film on the electrodes than either poly(**FFF**) or poly(**FMF**). These observed differences in film thickness and device coverage make the task of deciphering the "better" conductor even more difficult. These measurements are conducted under ambient conditions at very slow (5 mV/s) scan rates, so the polymers are more susceptible to degradation in their oxidized states.

Attenuated Total Reflectance Infrared (ATR-IR) Spectroscopy. The ATR-IR spectra of neutral undoped poly(**FMF**), poly(**FBF**), and poly(**FFF**) were obtained by first electrochemically growing the polymer of interest in an ITO glass electrode. The ATR-IR spectrum of the film was then taken. This can be achieved because the IR radiation only penetrates into the surface of the sample, and therefore the ITO glass does not interfere with the spectra obtained. The absence of carbonyl peaks in the spectra suggests that very little if any ring-opening occurred for all three polymers (Figure 7). However, under the present polymer growth conditions, we cannot rule out that the poly(**FFF**) neutral UV−vis peaks that persist upon oxidation are due to other types of furan defect structures formed during electropolymerization.

Conclusions

The new furan-containing monomer 2,7-bis(2-furanyl)-1,6-methano[10]annulene **FMF** was shown to have the highest λ_{max} of the bisfuranyl copolymers investigated. Additionally, it shares the least positive monomer oxidation potential with α-terfuran (**FFF**). The polymer formed from the methano[10]annulyl monomer also had the second least positive oxidation potential and the highest neutral polymer λ_{max} with the broadest peak. Poly(**FMF**)'s ATR-IR spectrum, like that of poly(**FBF**) and poly(**FFF**), suggests that during electropolymerization little or no ring-opening occurred, although spectroelectrochemical data indicate that the poly(**FFF**) has some localized electronic character relative to polymers containing the benzene or annulene fragments. Qualitative conductivity suggests that poly(**FMF**), poly(**FFF**), and poly(**FBF**) were indeed conductive in their oxidized and electrochemically doped states. Unique to poly(**FMF**) was the incredibly broad absorption profile observed in the oxidized conductive state. It is fair to deduce that 1,6-methano[10]annulene offers gentle electrosynthesis conditions for furan-based conductive polymers, with electronic properties that are comparable to other standard six π-electron (hetero)aromatics. We are presently investigating the chemical synthesis of these and other conjugated polymers that incorporate 1,6-methano[10]annulene to push these attributes into isolable and processable furan-based polymers.

Experimental Section

General Considerations. Reactions were performed in flame-dried glassware which had been cooled under nitrogen or argon and were maintained under an atmosphere of nitrogen or argon. Dimethylformamide (DMF) obtained from Aldrich was degassed by sparging with nitrogen or argon. Tetrakis(triphenylphosphine)palladium, $Pd(PPh_3)_4$, was obtained from Strem Chemicals. 1,6-Methano[10]annulene was synthesized using the procedures of Vogel et al.[24] 2,7-Dibromo-1,6-methano[10]-annulene was made by brominating the annulene with N-bromosuccinimide.[25] 1,5-Diiodonaphthalene was synthesized from 1,6-diaminonaphthalene (Acros) via the Sandmeyer reaction.[26] 2,5-Dibromofuran was synthesized as prepared by Keegstra et al.[27] All other chemicals were obtained from Aldrich and used without further purification. ^{1}H NMR and ^{13}C NMR spectra were obtained for samples in deuterated chloroform (the signal for residual protio solvent was set at 7.26 ppm for ^{1}H NMR and 77 ppm for ^{13}C NMR) using Bruker Avance 300 and 400 MHz FT-NMR spectrometers. Mass spectra were obtained using VG Instruments VG70S magnetic sector mass spectrometer, with EI and CI ionization.

UV−vis Spectroscopy. For each monomer, a solution of $\sim 3 \times 10^{-6}$ M in chloroform was used for obtaining the UV−vis spectra at room temperature. The instrument employed was the Varian Cary 50 UV−vis spectrophotometer.

Electrochemical Methods. Cyclic voltammetry and electrochemical polymerizations were carried out using an Autolab PGSTAT302 potentiostat/galvanostat. A 1.6 mm diameter platinum button was used as the working electrode for cyclic voltammetry. A Pt wire was used as the counter electrode, and an Ag wire in 0.01 M $AgNO_3$ and 0.1 M $TBAPF_6$ in MeCN was used as the quasi-internal reference electrode (Bioanalytical Systems). All electrochemical potentials are reported and discussed relative to this reference electrode. Acetonitrile and dichloromethane were dispensed after being pushed through two columns of activated alumina. Tetrabutylammonium hexafluorophosphate was obtained from Aldrich and recrystallized from ethanol prior to use. All electrolyte concentrations were 0.1 M and the monomer concentrations were 5 mM.

Qualitative in situ conductivity was also obtained using the above-mentioned instrument by utilizing the bipotentiostat settings. The working electrodes were Au interdigitated microelectrode arrays where the 15 μm electrode fingers were separated by 15 μm (Microsensor Systems, Inc.) while the counter and reference electrodes were the same as those mentioned above. Polymers were electropolymerized on the Au microelectrode device from a 5 mM solution of monomer in 0.1 M $TBAPF_6$/ACN. The cyclic voltammogram of the polymer was then recorded. Finally, drain current was measured within the same potential range as the CV was measured. A potential difference of 40 mV was applied between the two scanning working electrodes.

Spectroelectrochemical Measurements. Electropolymerization of the monomers was done using 70−100 Ω/sq surface resistivity indium-doped tin oxide (ITO) (Aldrich) as the working electrode and 0.1 M $TBAPF_6$ in CH_2Cl_2 as the electrolyte. The polymer-coated ITO was rinsed with fresh electrolyte and placed in a quartz cuvette containing blank electrolyte with counter and reference electrodes similar to those described above for cyclic voltammetry. While varying the potential at which the polymer was held, the UV−vis spectra were recorded using the Varian Cary 50 UV−vis spectrophotometer. A baseline of ITO in monomer-free electrolyte was used.

ATR-IR Spectroscopy. Polymer films were grown on ITO-coated glass electrodes from 5 mM solutions of monomer in 0.1 M $TBAPF_6$/ACN. These films were then examined using the Nexus 670 FT-IR.

Theoretical Calculations. The density functional theory B3LYP/6-31G* method was employed in Spartan to determine the HUMO and LUMO of the monomers.

2,7-Di(furan-2-yl)-1,6-methano[10]annulene (FMF). A 25 mL Schlenk tube was charged with 100 mg of 2,7-dibromo-1,6-methano[10]annulene (0.3 mmol) and 20 mg of $Pd(PPh_3)_4$ (0.02 mmol). The flask was evacuated and placed under argon. 2.5 mL of DMF was added, and the mixture was stirred to dissolve the solids. 250 mg (0.7 mmol) of 2-tributyltin furan at once was added, and the solution was heated to 80 °C and left to stir for 15 h. After cooling to room temperature, the reaction was diluted with ether (10 mL) and stirred vigorously 1 M KF solution (10 mL). The aqueous layer was removed and washed with 1 M KF solution (30 mL) and NH_4Cl (3 × 30 mL). The organic layer was dried over $MgSO_4$ and filtered, and the solvent was removed under reduced pressure. The product was purified by chromatography on a silica plug using hexane as the eluent. This yielded pure FMF (90 mg, 0.3 mmol, quant.) as a yellow solid. ^{1}H NMR (300 MHz, $CDCl_3$) δ: 7.88 (d, J = 7.2 Hz, 2H), 7.57 (s, 2H), 7.52 (d, J = 7.2 Hz, 2H), 7.17 (t, J = 7.2 Hz, 2H), 6.71 (s, 2H), 6.52 (m, 2H), −0.075 (s, 2H). ^{13}C NMR (100 MHz, $CDCl_3$) δ: 154.6, 142.7, 130.6, 130.1, 128.0, 125.1, 116.8, 111.7, 109.1, 35.6. HRMS (EI) calcd for $C_{19}H_{14}O_2$ [M^+]: 274.0994. Found: 274.0991.

1,5-Di(furan-2-yl)naphthalene (FNF). A 25 mL Schlenk tube was charged with 100 mg of 2,5-diiodonaphthalene (0.3 mmol) and 10 mg of $Pd(PPh_3)_4$ (0.01 mmol). The flask was evacuated and placed under argon. 2.5 mL of DMF was added, and the mixture was stirred to dissolve the solids. 200 mg (0.6 mmol) of 2-tributyltin furan was added at once, and the solution was heated to 80 °C and left to stir for 15 h. After cooling to room temperature, the reaction was worked up as for **FMF**. The product was purified by chromatography on a silica plug using hexane as the eluent. This yielded pure **FNF** (63 mg, 0.2 mmol, 93%) as a white solid. ^{1}H NMR (400 MHz, $CDCl_3$) δ: 8.38 (d, J = 8 Hz, 2H), 7.74 (d, J = 8 Hz, 2H), 7.64 (m, 2H), 7.55 (t, J = 8 Hz, 2H), 6.72 (dd, 2H), 6.60 (m, 2H). ^{13}C NMR (100 MHz, $CDCl_3$) δ: 153.5, 142.5, 131.1, 129.2, 126.5, 126.2, 125.9, 111.4, 109.5. HRMS (EI) calcd for $C_{18}H_{12}O_2$ [M^+]: 260.0837. Found: 260.0837.

1,4-Di(furan-2-yl)benzene (FBF)[15]**.** A 25 mL Schlenk tube was charged with 250 mg of 1,4-dibromobenzene (1.1 mmol) and 60 mg of $Pd(PPh_3)_4$ (0.05 mmol). The flask was evacuated and placed under argon. 3 mL of DMF was added, and the mixture was stirred to dissolve the solids. 801 mg (2.2 mmol) of 2-tributyltin furan was added at once, and the solution was heated to 80 °C and left to stir for 15 h. After cooling to room temperature, the reaction was worked up as for **FMF**. The product was purified by chromatograpy on a silica column using hexane as the eluent. This yielded pure **FBF** (170 mg, 0.82 mmol, 77%) as an off-white shiny solid. ^{1}H NMR (400 MHz, $CDCl_3$) δ: 7.69 (s, 4H), 7.48 (m, 2H), 6.67 (d, J = 4 Hz, 2H), 6.49 (m, 2H). HRMS (EI) calcd for $C_{14}H_{10}O_2$ [M^+]: 210.0681. Found: 210.0681.

2,5-Di(furan-2-yl)thiophene (FTF)[13]**.** A 25 mL Schlenk tube was charged with 250 mg of 2,5-dibromothiophene (1.0 mmol) and 60 mg of $Pd(PPh_3)_4$ (0.05 mmol). The flask was evacuated and placed under argon. 3 mL of DMF was added, and the mixture was stirred to dissolve the solids. 780 mg (2.2 mmol) of 2-tributyltin furan was added at once, and the solution was heated to 80 °C and left to stir for 15 h. After cooling to room temperature, the reaction was worked up as for **FMF**. The product was purified by chromatograpy on a silica column using hexane as the eluent. This yielded pure **FTF** (150 mg, 0.67 mmol, 65%) as a white solid. ^{1}H NMR (400 MHz, $CDCl_3$) δ: 7.41 (m, 2H), 7.17 (s, 2H), 6.51 (m, 2H), 6.45 (m, 2H). HRMS (EI) calcd for $C_{12}H_8O_2S$ [M^+]: 216.0245. Found: 216.0243.

2,2′,5′,5″-Terfuran (FFF)[12]**.** A 250 mL flask was charged with 550 mg of 2,5-dibromofuran (2.2 mmol) and 61 mg of $Pd(PPh_3)_4$ (0.05 mmol). The flask was evacuated and placed under argon. 25 mL of DMF was added, and the mixture was stirred to dissolve the solids. 1.7 g (4.9 mmol) of 2-tributylstannylfuran was added at once, and the solution was heated to 80 °C and left to stir for 15 h. After cooling to room temperature, the reaction was worked up as for **FMF**. Attempted to purify by chromatography on a column using hexane as the eluent but was unsuccessful. The product was then recrystallized from ethanol. This yielded pure **FFF** (51 mg, 0.25 mmol, 10%) as a yellow crystalline solid. ^{1}H NMR (400 MHz, $CDCl_3$) δ: 7.43 (s, 2H), 6.61 (s, 4H), 6.47 (s, 2H). HRMS (EI) calcd for $C_{12}H_8O_2S$ [M^+]: 200.0473. Found: 200.04721.

Acknowledgment. Johns Hopkins University and the NSF (CAREER: DMR-0644727) provided generous financial support.

Supporting Information Available: FTF electropolymerization, poly(**FTF**) cyclic voltammetry and spectroelectrochemical data, ^{1}H NMR for all monomers, and ^{13}C NMR for new monomers. This material is available free of charge via the Internet at http://pubs.acs.org.

References and Notes

(1) González-Tejera, M. J.; Sánchez, E.; Carrrillo, I. *Synth. Met.* **2008**, *158*, 165–189.
(2) Shilabin, A. G.; Entezami, A. A. *Eur. Polym. J.* **2000**, *36*, 2005–2020.
(3) Oshawa, T.; Kaneto, K.; Yoshino, K. *Jpn. J. Appl. Phys.* **1984**, *23*, L633–L665.
(4) Pan, W. L.; Song, J. G.; Chen, Y.; Wan, Y. Q.; Song, H. C. *Spectrochim. Acta, Part A* **2007**, *66*, 1300–1306.
(5) Hutchinson, G. R.; Zhao, Y. J.; Delley, B.; Freeman, A. J.; Ratner, M. A.; Marks, T. J. *Phys. Rev. B* **2003**, *68*, 035204.
(6) Armour, M.; Davies, A. G.; Upadhyay, J.; Wassermann, A. *J. Polym. Sci., Part A1* **1967**, *5*, 1527−1538.
(7) Gandini, A. *Adv. Polym. Sci.* **1977**, *25*, 47–96.
(8) Zotti, G.; Schiavon, G.; Comisso, N. *Synth. Met.* **1990**, *36*, 337–351.
(9) Lamb, B. S.; Kovacic, P. *J. Polym. Sci., Polym. Chem.* **1980**, *18*, 2423.
(10) Tourillon, G.; Garnier, F. *J. Electroanal. Chem.* **1982**, *135*, 173–178.
(11) Wan, X.; Yan, F.; Jin, S.; Liu, X.; Xue, G. *Chem. Mater.* **1999**, *11*, 2400–2407.
(12) Glenis, S.; Benz, M.; LeGoff, E.; Schindler, J. L.; Kannewurf, C. R.; Kanatzidis, M. G. *J. Am. Chem. Soc.* **1993**, *115*, 12519–12525.
(13) Galal, A.; Lewis, E. T.; Ataman, Y.; Zimmer, H.; Marrk, H. B. *J. Polym. Sci., Part A: Polym. Chem.* **1989**, *27*, 1891–1896.
(14) Joshi, M. V.; Helmer, C.; Cava, M. P.; Cain, J. L.; Bakker, M. G.; McKinley, A. J.; Metzger, R. M. *J. Chem. Soc., Perkin Trans.* **1993**, *2*, 1081–1086.
(15) Reynolds, J. R.; Child, A. D.; Ruiz, J. P.; Hong, S. Y.; Marynick, D. S. *Macromolecules* **1993**, *26*, 2095–2103.
(16) Hong, S. Y.; Marynick, D. S. *Macromolecules* **1992**, *25*, 3591–3595.
(17) Brillas, E.; Carrasco, J.; Centellas, F.; Cabot, P. L.; Fornaguera, J.; Garrido, J. A.; Rodriguez, R. M. *Synth. Met.* **2001**, *119*, 401–402.

(18) Yoneyama, H.; Kawabata, K.; Tsujimoto, A.; Goto, H. *Electrochem. Commun.* **2008**, *10*, 965–969.
(19) Doskocz, J.; Doskocz, M.; Roszak, S.; Soloducho, J.; Leszczynski, J. *J. Phys. Chem. A* **2006**, *110*, 13989–13994.
(20) Peart, P. A.; Tovar, J. D. *Org. Lett.* **2007**, *9*, 3041–3044.
(21) Peart, P. A.; Repka, L. M.; Tovar, J. D. *Eur. J. Org. Chem.* **2008**, *9*, 2193–2206.
(22) Kittlesen, G. P.; White, H. S.; Wrighton, M. S. *J. Am. Chem. Soc.* **1984**, *106*, 7389–7396.
(23) Ofer, D.; Crooks, R. M.; Wrighton, M. S. *J. Am. Chem. Soc.* **1990**, *112*, 7869–7879.
(24) Vogel, E.; Roth, H. D. *Angew. Chem., Int. Ed. Engl.* **1964**, *3*, 228–229.
(25) Vogel, E.; Böll, W. A.; Biskup, M. *Tetrahedron Lett.* **1966**, *7*, 1569–1575.
(26) Sondheimer, F. *Acc. Chem. Res.* **1972**, *5*, 81–91.
(27) Keegstra, M. A.; Klomp, A. J. A.; Brandsma, L. *Synth. Commun.* **1990**, *20*, 3371–3374.